

Optimization of Sensor Positions for Detecting Knock in Spark Ignition Engines

*L'optimisation des positions de capteurs pour la détection
du cliquetis dans les moteurs à explosion*



Abdelhak M. ZOUBIR and
Department of Electrical Engineering
Ruhr University Bochum, FRG

Abdelhak M. Zoubir was born in Algiers, Algeria, on June 21, 1958. He received the Diplom-Ingenieur degree in electrical engineering from Fachhochschule Niederrhein, Krefeld in April 1983 and from Ruhr University Bochum, Bochum, Germany in March 1987, respectively. Since 1987 he has served as a teaching and research assistant at Lehrstuhl für Signaltheorie, Ruhr University Bochum where he is working towards his doctorate. His current research interests include spectrum estimation, parameter estimation and detection, higher order spectral analysis and array signal processing.



Thomas M. BOSSMEYER ⁽¹⁾
Department of Electrical Engineering
Ruhr University Bochum, FRG

Thomas M. Bossmeyer was born in Westerholt/Westf., FRG, in 1961. In October 1982, he began a study of electrical engineering at Ruhr University, Bochum, FRG, with emphasis on communications, signal processing, and high-frequency engineering. After graduation in January 1988, he became a research assistant at Lehrstuhl für Signaltheorie, Ruhr University where he is working towards his doctorate. His research interests include analysis of machinery noise and vibration with main emphasis on the detection of knock in spark ignition engines.

ABSTRACT

In this study, we consider the problem of finding optimum sensor positions in a group of vibration sensors for knock detection. We propose a method that is less complex than holographic techniques because only signal processing and statistical tests are used. Our method is based on the linear prediction of an arbitrary sensor output from the remaining outputs in the sensor group. The relevancy of the sensor is thus characterized by the closeness to zero of the multiple coherence of its output with the remaining sensor outputs at some frequencies of interest. We choose a suitable statistic, approximate its distribution, and construct the generalized sequentially rejective Benferroni test. We have found in

an experiment that the sensor position proposed by the engine manufacturer is not optimum. Experiments with a digital signal processor-based system emphasize the usefulness of this procedure. Through this procedure, we show that the performance of knock detectors strongly depends on the position of the sensor in use and can be improved significantly with moderate effort.

KEY WORDS

Detection of Knock ; Resonance Modes ; Sensor Positions, Linear Prediction ; Multiple Coherence ; Bonferroni Multiple Test.

⁽¹⁾ Supported by Volkswagen AG, Wolfsburg, FRG.

RÉSUMÉ

Cette étude présente une approche permettant de déterminer les positions optimales de capteurs dans un groupe d'accéléromètres pour la détection du cliquetis dans un moteur à explosion. Cette approche est moins complexe que les méthodes holographiques car nous utilisons uniquement le traitement du signal et des tests statistiques. La méthode proposée est basée sur la prédiction linéaire du signal à la sortie d'un capteur à partir des signaux obtenus aux sorties des autres capteurs du groupe. Ainsi, l'emplacement optimal d'un capteur est caractérisé par la proximité de zéro de la cohérence multiple aux fréquences intéressantes. Nous avons choisis une statistique appropriée, approximé sa loi de répartition et appliqué le test multiple à rejet séquentiel de Bonferroni. Nous avons constaté dans

une expérience que la position de capteur proposée par le constructeur n'est pas optimale dans le groupe. Les résultats obtenus avec un système basé sur un processeur numérique de signaux accentuent l'utilité de cette approche. Ainsi, nous avons montré que la performance des détecteurs de cliquetis dépend fortement de l'emplacement de l'accéléromètre utilisé et peut être améliorée significativement sans grands efforts.

MOTS CLÉS

Détection du cliquetis ; modes de résonance ; positions de capteurs ; prédiction linéaire ; cohérence multiple ; test multiple de Bonferroni.

1. Introduction

The efficiency of a spark ignition engine, the favored engine of today's passenger cars, can be improved by an increase of its compression ratio. However, for high compression ratio engines the angle of ignition for minimum fuel consumption lies in a region where knock occurs. Knock is known as an abnormal combustion of the gas mixture causing rapid rise of temperature and pressure. This may lead to engine damage, particularly when it occurs at high speed. Knock detection systems with structural vibration sensors are used to control high compression engines for better fuel economy while avoiding engine damage as well as noise annoyance to the vehicle occupants.

The use of vibration sensors on the surface of the engine is easy and economical but makes the detection of knock difficult. This is due to the poor signal to noise power ratio (SNR) of the vibration signals. The performance of knock detection systems in use, e.g. [1], is nonoptimum because they are tuned to only one frequency band which causes a reduction of the SNR of the vibration signals. In this contribution, we present a detection scheme that is more sensitive than the current ones. We also discuss its implementation on a 16 bit fixed-point digital signal processor with real time capability.

Knock detectability can be improved if the vibration sensors are placed optimally on the engine surface. Holographic techniques for imaging knock centres have been proposed [2, 3], but their application is complicated and does not necessarily lead to a practical solution. Up to now, the sensor positions have been chosen heuristically. In this contribution, we present a method for finding optimum positions of sensors within a sensor group being positioned for example heuristically on the engine. The method is less complex than holographic techniques because only signal processing and statistical tests are used.

In section 2, we introduce the problem of knock and present the data model. In section 3, we propose a parametric detection scheme. Section 4 concerns the optimization of sensor positions for knock detection. A linear prediction approach is used to investigate the test of relevancy of sensors in a group. We discuss experimental results in section 5 before concluding.

2. Detection of Knock

2.1. THE PROBLEM

Since its invention more than 100 years ago, the performance of the spark ignition engine has been continuously improved. Special interest has been focused on a reduction of specific fuel consumption. In view of dwindling oil resources and growing air pollution, striving for increased efficiency seems to become even more important. Although diesel engines exhibit a somewhat higher efficiency, spark ignition (S.I.) engines are still preferred for use in passenger cars due to lower noise emissions and vibrations. An effective mean for lowering fuel consumption of S.I. engines is to increase the compression ratio. In spite of improvements in fuel quality and combustion chamber design [4, 5] further increase of compression is limited by the occurrence of knock, an extremely fast combustion that generates a knocking or ringing sound. In the past, two different theories were developed to explain knock. The first one states that knock is a result of flame acceleration, the second one states that pre-reactions in the unburnt part of the gas cause partial auto-ignition [6]. More recent studies by means of optical elements in the combustion chamber show that both mechanisms can generate knock [7, 8]. Knock results in rapid rise of temperature and pressure. The velocity of the flame front may exceed 2 000 m/s and high-frequency pressure fluctuations may reach 90 bar at extreme knock [8].

Frequent occurrence of knock has to be avoided because of its damaging effect on the engine, especially at high speed. At lower speed, knock is unwanted because of the annoyance to passengers. Knock also reduces efficiency due to heat loss resulting from turbulences in the combustion chamber. Corresponding power loss can reach up to 10 % at heavy knock [6]. Knock can be controlled by adapting the angle of ignition. For an engine with a high compression ratio, the angle of minimum fuel consumption is located in a region where knock occurs, and knock can be avoided only at the cost of decreased efficiency. The so-called knock limit is not fixed but depends, for example, on speed, load, fuel quality, and age. In addition, there also exist remarkable differences between the cylinders of one engine — due to worse cooling, the innermost ones in

general exhibit a higher sensitivity to knock. This means that to avoid engine damage, the angle of ignition has to be chosen with respect to worst conditions of each cylinder, which in turn significantly increases fuel consumption.

To attain safe operation at maximum efficiency, engine control systems which detect knock and adapt spark timing of each cylinder separately have found special interest [9, 1]. The performance of such systems suffers from the low SNR of the structural vibration signal that is taken by an acceleration sensor on the engine wall. Especially at high speed, noise from valves or bearings can mask knock and prohibit detection. In-cylinder pressure is preferred because of its high SNR but requires proper mounting of a pressure sensor in each cylinder. Corresponding costs restrict use of cylinder pressure to reference purposes in engine or fuel development, although proposals for application in production engine systems have been made [10]. The ionization current measured by the spark plug inside the combustion chamber may present a fair compromise between high SNR and low cost [11, 12] but this has to be verified by further investigation. Another paper [13] recently published proposes comparison of the actual noise level taken by a microphone with a reference level that depends on engine speed to detect knock. However, this method will probably not allow identification of the actual knocking cylinder.

A promising approach to improve the detection of knock at moderate costs is use of sophisticated signal processing methods to analyse structural vibrations. In the following section, we present a brief overview of a sensitive parametric detector developed by N. Härle [14]. The adjective *parametric* stems from the fact that the detector is based on a test statistic with few parameters that are sufficient for a complete description.

2.2. DATA AND SIGNAL MODEL

The rapid combustion of knocking cycles generates damped acoustical oscillations in the burnt gas [15]. For a cylindrical combustion chamber of bore $2R$ and height h filled with a homogeneous gas, the frequencies of the cavity resonances are known from theory [16]. The height varies with the position of the piston and so do the corresponding frequencies. Therefore, we restrict ourselves to circumferential and radial modes whose frequencies are given by

$$(1) \quad f_{m,n} = \frac{c\eta_{m,n}}{2\pi R}, \quad m, n \geq 1,$$

where $c = c_0 \sqrt{T}$ is the velocity of sound in the gas, T is the absolute temperature, and $\eta_{m,n}$ is the n -th zero of the first derivative of the Bessel function of the first kind and order m . Temperature and frequencies vary with crank angle γ in a well-known manner due to motion of the piston. If $T = T(\gamma)$ and γ_0 is a reference angle, then adiabatic expansion results in

$$(2) \quad \frac{T(\gamma)}{T(\gamma_0)} = \left(\frac{V(\gamma_0)}{V(\gamma)} \right)^{\delta-1}.$$

The adiabatic exponent is given by $\delta > 1$ and the combustion chamber volume by

$$(3) \quad V(\gamma) = V(0^\circ) + \pi R^2 s \left(1 - \cos \gamma + \frac{\ell}{s} - \sqrt{\left(\frac{\ell}{s} \right)^2 - \sin^2 \gamma} \right),$$

where s is the half stroke and ℓ the length of the driving rod.

As can be seen from the equations given above, the frequencies $f_{m,n}$ decrease monotonically during the expansion stroke. To compensate the resulting shift in frequency, Härle and Böhme [17] propose use of a time axis transformation leading to oscillations with constant frequencies. The transformation may be realized by non-equidistant sampling where the sampling intervals is not fixed but is varied in such a manner that the differences in phase of the oscillations are the same for any two successive sampling instants. This is possible because geometric data as s , R , and ℓ of an engine are known and the adiabatic exponent δ is approximately a constant that can be measured.

Pressure oscillations can be observed only after completion of the combustion when release of thermal energy has finished and the filling of the combustion chamber is approximately homogeneous. The corresponding crank angle depends on deterministic characteristics like spark timing and on random variations of the actual combustion process. For knocking cycles, this point is reached earlier than for non-knocking ones. The earlier the knock occurs the earlier combustion is completed and the corresponding knock intensity will be greater because a greater portion of unburnt gas has autoignited. The upper bound of the interval of observation is reached by damping effects due to heat loss. Therefore, the interval of interest to detect knock ranges from approximately 10° to 70° after top dead center.

We restrict our signal model to this interval and ignore all data outside. For convenience, we sort the frequencies of resonances in increasing order, normalize them with respect to the sampling frequency and a reference angle γ_0 , and denote them by f_p , $p = 1, \dots, P$. Denoting time instants by integers t , where $t = 0$ is the starting point of the interval of observation, superposition of P oscillations leads to

$$(4) \quad S(t) = \begin{cases} \sum_{p=1}^P A_p e^{-d_p t} \cos(\omega_p t + \Psi_p), & t = 0, 1, \dots \\ 0, & \text{else,} \end{cases}$$

where $\omega_p = 2\pi f_p$, and A_p , d_p , and Ψ_p are the amplitudes, damping constants, and phases of the oscillations, respectively.

For the purpose of knock detection or testing relevancy of a sensor, the model defined in (4) is simplified by the following reasonable assumptions. Data is available only in a small time interval and dampings may be neglected or compensated by an appropriate weighting function.

Amplitudes and phases are assumed to be independent random variables. We may then locally approximate the signal by a stationary stochastic process with spectral density $C_{SS}(\omega)$.

A model for structural vibrations of the engine housing follows immediately. We regard $r + 1$ acceleration sensors mounted at suitable locations on the engine wall and assume the transmission of oscillations inside the combustion chamber to the engine housing to be linear. This assumption seems to be reasonable because we have no theoretical evidence of a distinct form of non-linearity. In addition, general solutions are available for linear models that can be modified to fulfill our needs.

We denote the impulse response of the transmission path to sensor m by $h_m(t)$.

The output of sensor m is then given by

$$Z_m(t) = \sum_k h_m(k) S(t - k) + U_m(t), \quad (5)$$

$m = 1, 2, \dots, r + 1.$

$U_m(t)$ is a stationary process that is uncorrelated with $S(t)$ and takes into account noise from valves, bearings, etc. To simplify notation, we define the $(r + 1)$ -dimensional vector

$$Z(t) = \sum_k \mathbf{h}(k) S(t - k) + \mathbf{U}(t), \quad (6)$$

where $Z(t) = (Z_1(t), \dots, Z_{r+1}(t))'$, $\mathbf{h}(t) = (h_1(t), \dots, h_{r+1}(t))'$, and $\mathbf{U}(t) = (U_1(t), \dots, U_{r+1}(t))'$, respectively, and $'$ denotes transposition. A signal flow diagram for this model is given in figure 1.

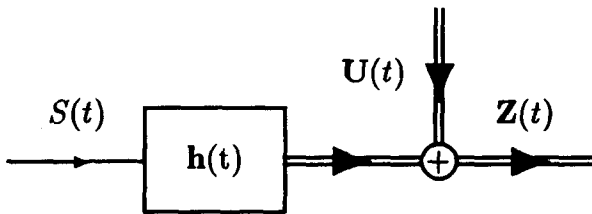


Fig. 1. — Multiple sensor signal flow diagram.

2.3. ASSUMPTIONS

We assume that the vector-valued series $Z(t)$, $t = 0, \pm 1, \dots$ is a stationary vector process with zero-mean and finite absolute moments of all orders. In addition the cumulant densities of $Z(t)$ of all orders are supposed to be continuous functions of frequencies. For example, we assume that the spectral density matrix $C_{ZZ}(\omega)$ is a smooth function of ω .

Let the time series data $Z(t)$, $t = 0, \dots, M - 1$ be available for n independent knocking combustion cycles and con-

sider the finite Fourier transform of length M of the ℓ -th cycle,

$$\mathbf{d}_Z^{(M)}(\omega, \ell) = \frac{1}{\sqrt{M}} \sum_{t=0}^{M-1} w\left(\frac{t}{M}\right) \mathbf{Z}(t, \ell) e^{-j\omega t} \quad (7)$$

for $\ell = 0, \dots, n - 1$. The function $w(u)$, $u \in \mathcal{R}$, is a smooth normalized window that vanishes for $u < 0$ and $u \geq 1$. Then it is known that for $\omega \neq 0 \pmod{\pi}$ the finite Fourier transforms $\mathbf{d}_Z^{(M)}(\omega, 0), \dots, \mathbf{d}_Z^{(M)}(\omega, n - 1)$ are independent and asymptotically identically complex normally distributed random vectors with zero mean and covariance matrix $C_{ZZ}(\omega)$ as $M \rightarrow \infty$ [18]. Define now

$$\mathbf{I}_{ZZ}^{(M)}(\omega, \ell) = \mathbf{d}_Z^{(M)}(\omega, \ell) \mathbf{d}_Z^{(M)}(\omega, \ell)^H,$$

where H denotes hermitian operation. Then the $\mathbf{I}_{ZZ}^{(M)}(\omega, \ell)$, $\ell = 0, \dots, n - 1$ are asymptotically $\mathcal{W}_{r+1}^C(1, C_{ZZ})$ distributed as $M \rightarrow \infty$, where $\mathcal{W}_{r+1}^C(1, C_{ZZ})$ denotes complex Whishart distribution of dimension $r + 1$ and degree of freedom 1. This suggests the estimate

$$\hat{C}_{ZZ}(\omega) = \frac{1}{n} \sum_{\ell=0}^{n-1} \mathbf{I}_{ZZ}^{(M)}(\omega, \ell),$$

where $\hat{}$ as in the sequel denotes an estimate. Under the conditions stated above, $\hat{C}_{ZZ}(\omega)$ is asymptotically $n^{-1} \mathcal{W}_{r+1}^C(n, C_{ZZ})$ distributed.

For the one-dimensional case, i.e. $r = 0$, $\mathbf{I}_{ZZ}^{(M)}(\omega, \ell)$ will be scalar and, under the assumptions noted above, its distribution may be approximated by a scaled chi-square-distribution with 2 degrees of freedom [18].

3. A Parametric Detector

We make no attempt to use multi-sensor processing to detect knock as proposed by Härle [14]. Instead, we use multiple sensors to find an optimum position for single-sensor knock detection. The amplitudes A_p of the signal model (4) are random variables that are stochastically greater for knocking cycles than for non-knocking ones. This fact is exploited in conventional detectors as well but it must be stressed that those detectors are tuned only to the lowest resonance frequency although the advantage of using higher frequencies has also been mentioned [15, 19]. Additional gain is reached by compensating the shift in frequency because resonance powers are then centered in relatively small bands and can be estimated at a higher SNR.

Figure 2 shows spectral estimates for cylinder pressure of selected cycles of the engine under test, a 3.4 l, 6 cylinder engine with electronic fuel injection and knock control. The upper curve represents an average of periodiograms of 11 knocking cycles, the lower (dotted) one an average of 11 non-knocking cycles, respectively. Data has been

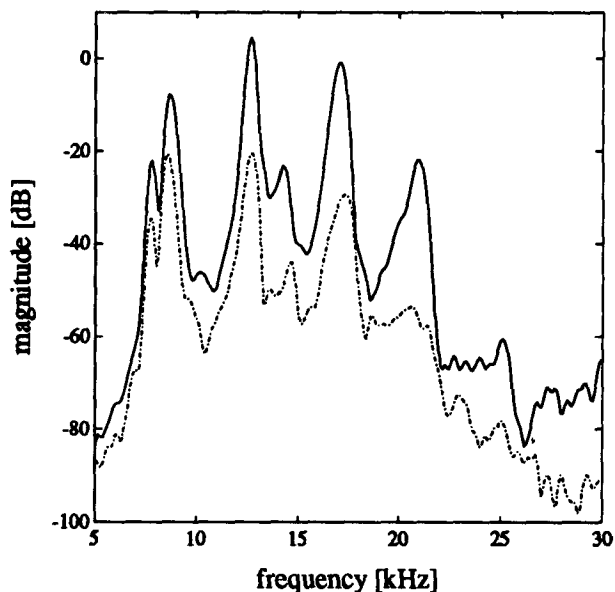


Fig. 2. — Spectral estimates for cylinder pressure of knocking (upper curve) and non-knocking cycles (lower curve).

transformed with respect to a reference crank angle $\gamma_0 = 0^\circ$ and windowed by a hanning window. The peaks of the resonances are clearly visible, however, there exist two peaks for the lowest mode. This may be due to *mode splitting* resulting from deviations of the actual combustion chamber geometry from an ideal cylinder. Hickling *et al.* [15] ascribe this effect to asymmetries caused by valves and spark plug holes. In general, temperature of the gas is only known up to a multiplicative factor which prohibits computation of resonance frequencies even for ideal engine geometries. However, the ratio of any two frequencies is independent of the actual level of temperature and may be used to check predictions based on theory. If one assumes such a temperature that the lowest peak of the periodogram of knocking cycles coincides with the lowest resonance frequency theoretical frequencies are 7.6, 12.5, 15.8, 17.3, 21.9, and 22.0 kHz, respectively. Locations of maxima of knocking cycles in figure 2 are 7.6, 8.7, 12.5, 14.3, 16.9, and 21.0 kHz. In general, agreement between theoretical and empirical frequency is quite good because of the simple engine geometry. However some resonances seem to be more affected by deviations from ideal cylindrical geometry. There also exist small differences between locations of maxima of knocking and non-knocking cycles, respectively. This may be attributed to additional heat loss during expansion of knocking cycles causing a systematic shift towards lower frequencies.

For modern engines with more complex shaped combustion chambers, for example those with a piston bowl as discussed in [20], deviations from ideal cylindrical geometry may be great and an analytical solution for the frequencies will not be available. In these cases where even the ratios of different frequencies are unknown and can therefore not be used to identify relevant peaks, resonance frequencies solely may be gained from spectral

estimates or finite-element computations. Additional difficulties arise in the case of structural vibration signals that contain many other narrow-band components. The transfer characteristics of the engine housing vary strongly with frequency and may cause differences between peaks of pressure and vibration spectra. The estimation of the coherence function as discussed in the following section may facilitate identification of relevant spectral components for the detection of knock.

An adaptive weighting function is applied to structural vibration data in the time domain. Adaptation is performed with respect to periodic events like opening or closing of valves that may generate strong impulses during the interval of observation. For example, for the engine under consideration the inlet valve of cylinder 1 opens at 146° after top dead center which corresponds to 26° after top dead center with respect to cylinder 5. As proposed by [14], the weight $w(t, l)$ of the t -th sample $y(t, l)$ of the l -th combustion is inversely proportional to the estimated root-mean-square (RMS) value $\sqrt{\overline{y(t, l)^2}}$ where $\overline{y(t, l)^2}$ is an average of $y(t, k)^2$, $k < l$ of non-knocking combustion cycles of the past. For non-knocking cycles the observed vibration signal $y(t, l)$ almost solely consists of noise and the estimated RMS value will approximately equal that of the noise. Clearly, $w(t, l)$ will be great for time instants t with a small root-mean-square value which means there will be low noise, and vice versa.

Estimation of power at resonance frequencies can be done by computing the periodogram or digitally filtering and integrating the squared filter output, whatever is appropriate. Smoothing in the frequency domain is highly recommended because of frequency fluctuations that are caused by cycle-to-cycle variations of the combustion process. In addition, a systematic shift in frequency for knocking cycles is caused by a decrease in temperature due to greater heat loss.

A weighted average T of estimated resonance powers is used to test for knock where the estimates $\hat{E}(\omega_p)$, $p = 1, \dots, P$ are computed by smoothing the periodogram over some frequencies in the vicinity of ω_p . The weights g_p are proportional to the relative difference of power in bands around resonance frequencies ω_p of knocking and non-knocking cycles, respectively. If we exploit asymptotic properties of the periodogram as indicated in subsection 2.3, the test statistic T may be approximated by a scaled chi-square-distributed random variable [14],

$$(8) \quad T = \sum_{p=1}^P g_p \hat{E}(\omega_p) \sim a \chi_b^2.$$

In (8), a is an unknown scaling factor and b is the unknown number of degrees of freedom of the distribution. It is well-known that the sum of P mutually independent chi-square-distributed random variables with n_p , $p = 1, \dots, P$ degrees of freedom each will be chi-square-distributed with $\sum_{p=1}^P n_p$ degrees of freedom [21]. If there exist any dependencies between the variates or they are differently

scaled the number of degrees of freedom will be less than $\sum_{p=1}^p n_p$. The parameters a and b can be found by estimating first and second order moments of T . A decision for knock is made if T exceeds a threshold κ that is chosen with respect to the acceptable rate of false alarms. A false alarm is a decision for knock if the actual cycle was in fact a non-knocking one. The rate of false alarms is of special importance because each decision on knock leads to an adaptation of the angle of ignition towards less knock thereby lowering the engine's efficiency. An inappropriate rate of false alarms therefore causes an unwanted increase in fuel consumption whereas single knocking cycles that are not detected will not destroy the engine.

Figure 3 summarizes the structure of the knock detector. After non-equidistant sampling and A/D-converting the vibration signal is adaptively weighted in the time domain (TW). The resonance powers of certain resonance frequencies are estimated (PE), adaptively weighted and averaged (FW). The sum is compared with an adaptively controlled threshold (TEST).

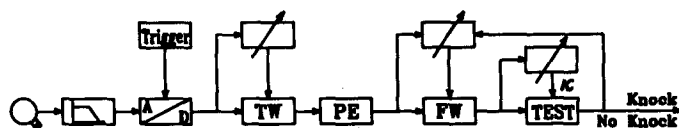


Fig. 3. — Signal flow diagram of the parametric detector.

Due to the availability of fast and cheap digital signal processors (DSP), the parametric detector is capable of real-time performance at moderate costs. Adaptation to a specific engine is done by updating a few parameters like frequencies, damping constants etc. For the engine under consideration in this paper, this is shown by experimental results in section 5. Experimental results of knock detection for a 4-cylinder engine with a more complicated combustion chamber using floating-point and fixed-point DSPs have been given [20]. A comparison between a FFT-based and a filter-based version of the parametric detector is completed by results of a non-parametric detector.

4. Optimization of Sensor Positions for Knock Detection

Holographic interferometry has been applied for many years as a diagnostic means in sound and vibration analysis [22]. Especially, the double pulsed laser holography has been proposed for imaging knock centres on an engine wall [2, 3]. It is based on two holograms that are taken by two laser light flashes in an interval of 0.1 to 1 ms. The simultaneous reconstruction of the two holograms generates a system of interference fringes on the surface of the engine. In this way, it is possible to visualize the vibration pattern of the engine excited by knock. For the application of these methods, however, the output of a vibration

sensor fixed on the engine wall in the vicinity of a vibration centre is connected with the trigger input of the laser system. It is obvious that in addition to the great deal of equipment required when using these methods, problems arise if more than one resonance mode frequency are to be considered.

In this section, we propose a method for finding optimum positions in a group of vibration sensors for detecting knock in combustion engines. It differs from holographic techniques in that only signal processing and statistical tests are used.

4.1. A PREDICTION FILTER APPROACH

In the sequel, we shall be concerned with the dimension reduction of the vibration sensor output $\mathbf{Z}(t)$, leading to outputs of sensors that are suitably positioned for knock detection. In the approach presented, we do not explicitly use the signal model given in (4), but the fact that only some frequencies are to be considered for detecting knock.

$\mathbf{Z}(t)$ from (6) is a $(r + 1)$ vector-valued stationary series with spectral density matrix

$$(9) \quad \mathbf{C}_{ZZ}(\omega) = \mathbf{H}(\omega) \mathbf{C}_{SS}(\omega) \mathbf{H}(\omega)^H + \mathbf{C}_{UU}(\omega).$$

Here, $\mathbf{H}(\omega) = \sum_t \mathbf{h}(t) \exp(-j\omega t)$ denotes the transfer

function matrix, and $\mathbf{C}_{UU}(\omega)$ the spectral density matrix of the $(r + 1)$ vector-valued noise process $\mathbf{U}(t)$. It is seen that the noise spectral density matrix $\mathbf{C}_{UU}(\omega)$, assuming $\mathbf{C}_{SS}(\omega) \neq 0$ and $\mathbf{C}_{ZZ}(\omega)$ to be positive definite at any ω , is related to the output spectral density matrix $\mathbf{C}_{ZZ}(\omega)$ by

$$\mathbf{C}_{UU}(\omega) = \mathbf{C}_{ZZ}(\omega)^{1/2} (\mathbf{I}_{r+1} - \mathbf{R}_{ZS}(\omega)) \mathbf{C}_{ZZ}(\omega)^{1/2}.$$

Herein, \mathbf{I}_{r+1} denotes the identity matrix of dimension $r + 1$ and

$$(10) \quad \mathbf{R}_{ZS}(\omega) = \mathbf{C}_{ZZ}(\omega)^{-1/2} \mathbf{C}_{ZS}(\omega) \mathbf{C}_{SS}(\omega)^{-1} \times \mathbf{C}_{SZ}(\omega) \mathbf{C}_{ZZ}(\omega)^{-1/2}$$

is a complex measure of the linear association of $\mathbf{Z}(t)$ with $\mathbf{S}(t)$ at frequency ω . Considering one component $Z_i(t)$ of the vector $\mathbf{Z}(t)$, (10) is reduced to the coherence function of $\mathbf{S}(t)$ with $Z_i(t)$ at frequency ω ,

$$(11) \quad |\mathbf{R}_{SZ_i}(\omega)|^2 = \frac{|C_{SZ_i}(\omega)|^2}{C_{SS}(\omega) C_{Z_i Z_i}(\omega)}, \quad i = 1, \dots, r + 1,$$

where $C_{SZ_i}(\omega)$ denotes the cross spectrum of $\mathbf{S}(t)$ with $Z_i(t)$. The coherence function $|\mathbf{R}_{SZ_i}(\omega)|^2$ takes values between zero and unity for any ω . The lower the noise, the closer coherence is to unity. The signal to noise power ratio of the vibration signal of sensor i at frequency ω is then given by

$$\frac{|\mathbf{R}_{SZ_i}(\omega)|^2}{1 - |\mathbf{R}_{SZ_i}(\omega)|^2}.$$

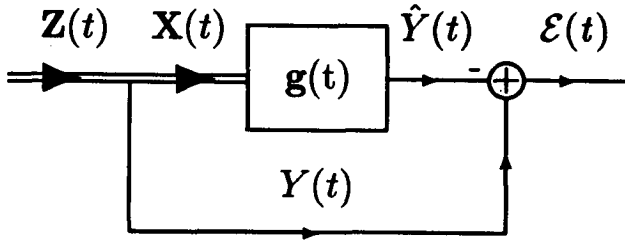


Fig. 4. — Linear prediction of $Y(t)$ from $X(t)$.

Let the $(r + 1)$ vector-valued stationary series $Z(t)$, $t = 0, \pm 1, \dots$, be partitioned into two series, $Z(t) = (X(t)', Y(t)')$ with $X(t)$ r vector-valued, and have spectral density matrix

$$C_{ZZ}(\omega) = \begin{pmatrix} C_{XX}(\omega) & C_{XY}(\omega) \\ C_{YX}(\omega) & C_{YY}(\omega) \end{pmatrix}.$$

$Y(t)$ is the output of the sensor of which relevancy for knock detection is to be tested within the group of sensors with output $Z(t)$. Based on the extent to which $Y(t)$ is determinable from $X(t)$ by linear time invariant operations, we shall decide the relevancy of the sensor with output $Y(t)$.

The methods of predicting $Y(t)$ from $X(t)$ linearly are well known [18]. Let $Y(t)$ be approximated by $\hat{Y}(t)$, and $\varepsilon(t)$ denotes the error series,

$$\varepsilon(t) = Y(t) - \hat{Y}(t) = Y(t) - \sum_u g(u) X(t - u).$$

The $g(t)$ that minimizes the variance $E\varepsilon(t)^2$ of the error series is given by

$$g(t) = \int_{-\pi}^{\pi} G(\omega) e^{j\omega t} \frac{d\omega}{2\pi},$$

where

$$G(\omega) = C_{YX}(\omega) C_{XX}(\omega)^{-1},$$

provided the required inverse exists. This leads to the error spectrum

$$(12) \quad C_{\varepsilon\varepsilon}(\omega) = (1 - |R_{YX}(\omega)|^2) C_{YY}(\omega),$$

where

$$(13) \quad |R_{YX}(\omega)|^2 = \frac{C_{YX}(\omega) C_{XX}(\omega)^{-1} C_{XY}(\omega)}{C_{YY}(\omega)}$$

is the multiple coherence of $Y(t)$ with $X(t)$ at frequency ω . It is the proportion of power of $Y(t)$ at frequency ω which is explained by the linear relationship with $X(t)$. It is seen from (12) that $|R_{YX}(\omega)|^2 = 0$ corresponds to the incoherent case in which $X(t)$ does not reduce the error variance. The value $|R_{YX}(\omega)|^2 = 1$ corresponds to the perfectly coherent case in which the error series is reduced

to zero. Thus, the closer the multiple coherence $|R_{YX}(\omega)|^2$ is to zero, the less is $Y(t)$ linearly predictable from $X(t)$ at frequency ω . Thus, the closeness to zero of $|R_{YX}(\omega)|^2$ at some frequencies of interest is a relevancy measure of the sensor with output $Y(t)$ in the group with output $Z(t) = (X(t)', Y(t)')$. In the sequel, we shall construct tests for measuring the closeness to zero of $|R_{YX}(\omega)|^2$ at the resonance frequencies.

4.2. RELEVANCY TESTS

Let the time series data $Z(t)$, $t = 0, \dots, M - 1$ be available for n combustion cycles. The spectral estimate $\hat{C}_{ZZ}(\omega)$ for $C_{ZZ}(\omega)$ is calculated by averaging n periodograms. We partition $Z(t) = (X(t)', Y(t)')$ and estimate $|R_{YX}(\omega)|^2$ by $|\hat{R}_{YX}(\omega)|^2$ obtained from (13) when the spectra are replaced by their estimates. Following the discussion given in the preceding subsection, we may test the relevancy of the sensor with output $Y(t)$ within the sensor group by testing the hypothesis

$$H_0 : |R_{YX}(\omega)|^2 \leq |R_{YX}^0(\omega)|^2$$

against

$$(14) \quad K_0 : |R_{YX}(\omega)|^2 > |R_{YX}^0(\omega)|^2.$$

$|R_{YX}^0(\omega)|^2$ is a suitably chosen bound in the interval $(0, 1)$. The test rejects H_0 if, for a given level of significance α , the test statistic is too large [23]. (14) suggests the sample multiple coherence $|\hat{R}_{YX}(\omega)|^2$ as a test statistic. Therefore, we shall first discuss the statistical properties of $|\hat{R}_{YX}(\omega)|^2$.

For the sake of simplicity, we drop the argument variable ω . Let \hat{R}^2 and R^2 denote the sample and the true multiple coherence, respectively. The limiting density function of \hat{R}^2 has been discussed in [24]. If the assumptions of subsection 2.3 are fulfilled it is given for $\omega \neq 0, \pm \pi$ and $0 \leq \hat{R}^2, R^2 \leq 1$, by

$$(15) \quad \frac{(1 - R^2)^n \cdot {}_2F_1(n, n; r; R^2 \cdot \hat{R}^2) \cdot \hat{R}^{2r-2} \cdot (1 - \hat{R}^2)^{n-r-1}}{B(n-r, r)},$$

where ${}_2F_1(\dots; \dots)$ is the confluent hypergeometric function and $B(\dots)$ is the beta function. It is seen from (15) that under the hypothesis $R^2 = 0$ the statistic $(n-r) \hat{R}^2 / r(1 - \hat{R}^2)$ has the F distribution with $2r$ and $2(n-r)$ degrees of freedom. In our case, it makes more sense to test the smallness of R^2 rather than $R^2 = 0$ because the latter means that $Y(t)$ and $X(t)$ are incoherent at the frequencies of interest. This can only occur if the sensor with output $Y(t)$ is not suitably positioned. However, there are no extensive tabulations for $R^2 \neq 0$. For $r = 1$ the tables of Amos and Koopmans [25] may be used. In [26] the upper and lower bounds to an equal tail areas confidence interval for R^2 have been calculated for some r, \hat{R}^2 and $n-r$ values and confidence coefficients $1 - \alpha$ with $\alpha = 0.05$ and $\alpha = 0.01$. However, the results

are not useful for testing an hypothesized value of R^2 .

The density function (15) is that of the squared multiple correlation coefficient of one real normal variate with $2r$ other real normal variates when computed from $2n$ observations without mean correction [27]. Roughly speaking, we may refer to the multiple coherence as a « squared multiple correlation coefficient in the frequency domain ». Thus, known results about the squared multiple correlation coefficient may be applied with slight modifications to the multiple coherence. In [28], we have used the test statistic

$$(16) \quad \hat{\Gamma}^2 = \frac{\hat{R}^2}{1 - \hat{R}^2},$$

and approximated its distribution to the F distribution, where we have fitted the first three moments of $\hat{\Gamma}^2$ to the corresponding moments of the assumed distribution (see also [29] for the squared multiple correlation coefficient). Thus, upper α points of $\hat{\Gamma}^2$ are derived from the F table. In this contribution, we use Fisher's normalizing z-transformation that has been proposed for the multiple correlation coefficient in [30]. Results of an empirical study to develop a similar normalizing transformation for the sample multiple coherence have been described in [31]. Enochson and Goodman suggested to approximate the distribution of $\tanh^{-1}|\hat{R}_{YX}(\omega)|$ by the normal distribution with mean

$$(17) \quad \tanh^{-1}|\hat{R}_{YX}(\omega)| + \frac{r}{4(n-r)} \times \left(1 + \frac{1}{\tanh^{-1}|\hat{R}_{YX}(\omega)| + 0.1} \right)$$

and variance $1/2(n-1)$ for $r=1$ and $1/2(n-r+1)$ for $r>1$.

The advantages of this approximation are its variance-stabilizing effects and that critical regions for testing hypothesized values of $|\hat{R}_{YX}(\omega)|^2$ are derived from tables of the normal distribution. It should be noted that many authors use the simpler mean of the approximate distribution $\tanh^{-1}|\hat{R}_{YX}(\omega)| + r/2(n-r)$ instead of (17). This approximation is not accurate for small $|\hat{R}_{YX}(\omega)|$, however, the assumed bias does not depend on $|\hat{R}_{YX}(\omega)|$.

The single hypothesis (14) tests the coherence at one frequency. Because in knock detection P frequencies are of interest, the test is not suitable in this form. It would lead to a relevancy decision only if the coherence to be tested for an arbitrary sensor is smaller than the coherences for testing the remaining sensors at all P frequencies. Also, because of the signal model given in (4), coherences at frequencies in the neighborhood of the resonance frequencies have to be considered. This motivates testing simultaneously the hypotheses $H_{1,-m}, \dots, H_{1,m}, \dots, H_{P,-m}, \dots, H_{P,m}$ and H , where

$$(18) \quad H: \bigcap_{p=1}^P \bigcap_{k=-m}^m H_{p,k}, \quad H_{p,k}: |\hat{R}_{YX}(\omega_{p,k})|^2 \leq |\hat{R}_{YX}^{p,k}|^2,$$

against one-sided alternatives. $|\hat{R}_{YX}^{p,k}|^2$ are suitably chosen

bounds, and $\omega_{p,k}$, $k = -m, \dots, m$, are frequencies in the neighborhood of the resonance frequencies ω_p with $\omega_{p,0} = \omega_p$, $p = 1, \dots, P$. From a heuristic point of view, we have used in [28] the mean of $\hat{\Gamma}^2$ over $(2m+1)P$ frequencies as a test statistic and approximated its distribution for testing the hypotheses in (18). For a given level of significance α , we have rejected H if the test statistic is too large.

Using the test statistics $\tanh^{-1}|\hat{R}_{YX}(\omega_{p,k})|$, $p = 1, \dots, P$, $k = -m, \dots, m$, we apply now Holm's sequentially rejective Bonferroni multiple test [32, 33]. For the sake of simplicity, let the hypotheses $H_{1,-m}, \dots, H_{1,m}, \dots, H_{P,-m}, \dots, H_{P,m}$ be denoted by H_1, H_2, \dots, H_N with associated statistics T_1, T_2, \dots, T_N , where $N = (2m+1)P$. Define by \mathcal{P}_i the significance probability of the test statistic T_i that is

$$P(T_i \geq t_i | H_i), \quad i = 1, \dots, N,$$

where t_i is the observed value of T_i . Once the \mathcal{P} -values of the test statistics for the H_i , $i = 1, \dots, N$ have been calculated, the sequentially rejective Bonferroni procedure can be implemented as follows: Order the \mathcal{P} -values $\mathcal{P}_{(1)} \leq \mathcal{P}_{(2)} \leq \dots \leq \mathcal{P}_{(N)}$ and let $H_{(1)}, H_{(2)}, \dots, H_{(N)}$ be the corresponding hypotheses. First check if $\mathcal{P}_{(1)} \leq \alpha/N$, in which case reject $H_{(1)}$ and proceed to test $H_{(2)}$; otherwise retain all the hypotheses and therefore H without further tests. Next check if $\mathcal{P}_{(2)} \leq \alpha/(N-1)$, in which case reject $H_{(2)}$ and proceed to test $H_{(3)}$; otherwise retain $H_{(2)}, \dots, H_{(N)}$ without further tests, and so on.

In (18) we have chosen bounds $|\hat{R}_{YX}^{p,k}|^2$ that may differ from one frequency to another. This enables us to obtain higher critical values for less important hypotheses and smaller critical values for the most important hypotheses. An alternative way to weight the hypotheses is to take a common bound, say $|\hat{R}_{YX}^0|^2$, and to apply the generalized sequentially rejective Bonferroni test [32]. Let as before H_1, H_2, \dots, H_N be the hypotheses to be tested and $\mathcal{P}_{(1)} \leq \mathcal{P}_{(2)} \leq \dots \leq \mathcal{P}_{(N)}$ be the obtained levels of the statistics T_1, T_2, \dots, T_N . Further let c_1, c_2, \dots, c_N be positive constants indicating the importance of the hypotheses in the sense that the constants corresponding to more important hypotheses are greater than those corresponding to less important ones. Introduce $\mathcal{S}_k = \mathcal{P}_k/c_k$ for $k = 1, 2, \dots, N$. The generalized sequentially rejective Bonferroni procedure can be implemented as follows: Order $\mathcal{S}_{(1)} \leq \mathcal{S}_{(2)} \leq \dots \leq \mathcal{S}_{(N)}$ and let $H_{(1)}, H_{(2)}, \dots, H_{(N)}$ and $c_{(1)}, c_{(2)}, \dots, c_{(N)}$ be the corresponding hypotheses and constants, respectively. First check if $\mathcal{S}_{(1)} \leq \alpha / \sum_{k=1}^N c_{(k)}$, in

which case reject $H_{(1)}$ and proceed to test $H_{(2)}$; otherwise retain all the hypotheses and therefore H without further tests. Next check if $\mathcal{S}_{(2)} \leq \alpha / \sum_{k=2}^N c_{(k)}$, in which case reject

$H_{(2)}$ and proceed to test $H_{(3)}$; otherwise retain $H_{(2)}, \dots, H_{(N)}$ without further tests, and so on. The generalized sequentially rejective Bonferroni multiple procedure is schematically described in figure 5. This test implies an increase of power for alternatives with high

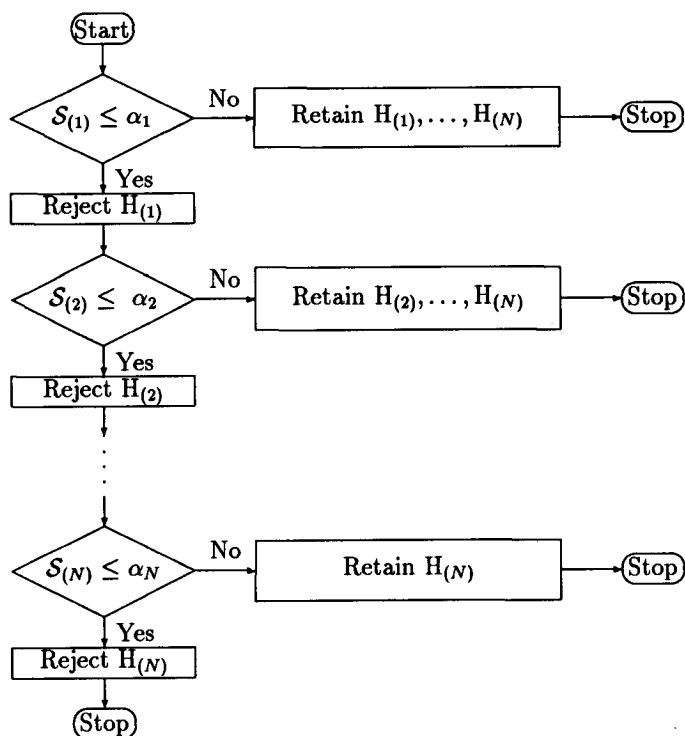


Fig. 5. — Schematic description of the generalized sequentially rejective Bonferroni test. α_j denotes $\alpha / \sum_{k=j}^N c_{(k)}$, $j = 1, \dots, N$.

values of c_k at the cost of decrease of power for alternatives to hypotheses with small values of c_k . It is noted that this test reduces to the former when all c_k are equal.

5. Experimental Results

5.1. TEST EQUIPMENT AND DATA PREPARATION

Experiments were performed using a 3.4 l, 6 cylinder engine with production knock control system. The high-pass filtered pressure signal of cylinder 5 ($S(t)$ in fig. 6) was recorded by an instrumentation tape recorder together with the output of four acceleration sensors. Two of these sensors (sensors with outputs $Z_1(t)$ and $Z_4(t)$ in fig. 6) had been mounted at the places of the standard sensors, the other ones at heuristically chosen positions on the engine wall. Figure 6 schematically shows these positions.

The engine was running at 1 750 rpm and at full load. Medium knock intensity was adjusted by an ignition angle of 22° before top dead center. One hundred digitized cycles were chosen for our analyses. In order to identify knocking cycles, we compared the difference between successive samples of the cylinder pressure signal at an interval ranging from 10 to 40° crank angle with a suitably chosen threshold. This method, proposed by Härle [14], exploits the fact that knock results in a steep pressure rise.

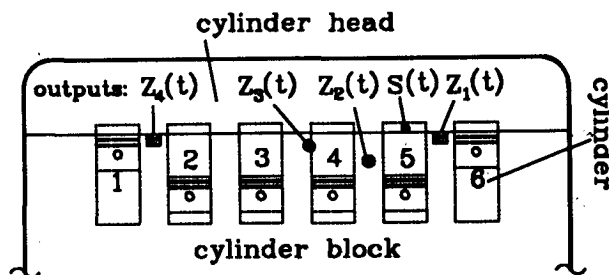


Fig. 6. — Sensor positions on the engine.

The decision was verified by visual inspection of the corresponding pressure signal. In this way, 11 cycles out of the 20 with highest power were found.

Resonance frequencies were estimated by averaging periodograms of the knocking cycles of $S(t)$ and smoothing over 3 frequency bins. Spectral peaks were found at 7.6, 8.7, 12.5, 16.9 and 21.0 kHz. The two peaks in the low-frequency part of the spectrum appear probably due to mode splitting. In contrast to other authors who have investigated such phenomena by computing an average of both frequencies [15], we decided to use the lower one. This decision is based on the estimated SNR of the acceleration sensor outputs that is maximum at 7.6 kHz. Similarly, $\hat{C}_{ZZ}(\omega)$ was obtained as $\hat{C}_{SS}(\omega)$.

5.2. OPTIMIZATION OF SENSOR POSITIONS

In this subsection, we present results of the generalized sequentially rejective Bonferroni test described in subsection 4.2. We apply the test on four modes ($P = 4$) and six neighboring frequencies ($m = 3$) where the difference between two adjacent frequencies equals 212 Hz. We consider the mode frequencies given in subsection 5.1. The weights c_1, \dots, c_N with $N = (2m + 1)P$ are chosen as follows :

$$(19) \quad (c_1, \dots, c_N)' = (c_{-m}, \dots, c_m, c_{-m}, \dots, c_m, c_{-m}, \dots, c_m, \dots, c_{-m}, \dots, c_m)'$$

where

$$(20) \quad c_k = \frac{\mu_k}{\sum_{k=-m}^m \mu_k}, \quad k = -m, \dots, m,$$

and the weights μ_k are those of the Parzen window of length $2m + 3$ [34]. Equation (19) means that the hypotheses $H_{p,-k}$ and $H_{p,k}$, as well as $H_{l,k}$ and $H_{l,-k}$ are weighted identically for $l, p = 1, \dots, P$, $k = -m, \dots, m$, and $l \neq p$. Up to now, no physical motivation has existed to weight the modes at the center frequencies ω_p differently. The choice of Parzen window is motivated by the fact that μ_k falls rapidly but smoothly when $|k|$ increases.

The relevancy decision for a sensor in a group is based on the linear predictability of the sensor output from the remaining sensor outputs. However, this may lead to a wrong result when a sensor with a very low SNR is used in the sensor group [28]. To prevent this occurrence, it is necessary to perform a two-stage test. At the first stage, sensors with low SNR have to be removed from the group. Thus, we test for $i = 1, \dots, r + 1$ the hypotheses $H_{1, -m}^i, \dots, H_{1, m}^i, \dots, H_{p, -m}^i, \dots, H_{p, m}^i$ and H^i , where

(21)

$$H^i : \bigcap_{p=1}^P \bigcap_{k=-m}^m H_{p, k}^i, H_{p, k}^i : |R_{SZ_i}(\omega_{p, k})|^2 \geq |R_{SZ_i}^0|^2,$$

against one-sided alternatives. The test (21) was applied at a level of significance $\alpha = 5\%$. The ordered scaled significance probabilities $\mathcal{S}_{(1)}$ to $\mathcal{S}_{(N)}$ are given in Table 1 for each statistic $\tanh^{-1} |\hat{R}_{SZ_i}(\omega_{p, k})|$, denoted by $S(t)|Z_i(t)$, $i = 1, \dots, 4$. Note that for the test (21) we obtain the \mathcal{P} -values by interchanging inequalities in the definition given in subsection 4.2. α_j stands for $\alpha / \sum_{k=j}^{28} c_{(k)}$,

where $j = 1, \dots, 28$ and $c_{(k)}$ are the corresponding hypotheses weights. It can be seen from Table 1 that the hypotheses H_i are rejected for all $i = 1, \dots, 4$ when $|R_{SZ_i}^0|^2 = 0.5$. Especially for $Z_4(t)$, all hypotheses $H_{p, k}$, $p = 1, \dots, 4$, $k = -3, \dots, 3$ are rejected.

Therefore, we remove $Z_4(t)$ and consider in the next stage the sensor group with output $Z(t) = (Z_1(t) Z_2(t) Z_3(t))'$. We give the ordered scaled significance probabilities $\mathcal{S}_{(1)}$ to $\mathcal{S}_{(28)}$ in Table 2. The hypotheses' weights and α are chosen as before, where $|R_{YX}^0|^2 = 0.31$. We see from

TABLE 1

Ordered \mathcal{P} -values of the statistics $\tanh^{-1} |\hat{R}_{SZ_i}(\omega_{p, k})|$ for testing (19) at a level of significance $\alpha = 5\%$ and $|R_{SZ_i}^0|^2 = 0.5$. Boldfaced numbers correspond to hypotheses that are not rejected.

j	α_j	$S(t) Z_1(t)$	α_j	$S(t) Z_2(t)$	α_j	$S(t) Z_3(t)$	α_j	$S(t) Z_4(t)$
1	0.0125	0.0000	0.0125	0.0000	0.0125	0.0000	0.0125	0.0000
2	0.0133	0.0000	0.0125	0.0000	0.0128	0.0000	0.0133	0.0000
3	0.0136	0.0000	0.0128	0.0000	0.0136	0.0000	0.0146	0.0000
4	0.0139	0.0000	0.0128	0.0000	0.0139	0.0000	0.0150	0.0000
5	0.0140	0.0000	0.0131	0.0000	0.0140	0.0000	0.0161	0.0000
6	0.0140	0.0000	0.0132	0.0000	0.0140	0.0000	0.0166	0.0000
7	0.0154	0.0000	0.0140	0.0000	0.0150	0.0000	0.0166	0.0000
8	0.0158	0.0000	0.0144	0.0000	0.0154	0.0000	0.0187	0.0000
9	0.0163	0.0000	0.0147	0.0000	0.0166	0.0000	0.0188	0.0000
10	0.0176	0.0000	0.0148	0.0000	0.0187	0.0000	0.0206	0.0000
11	0.0177	0.0000	0.0148	0.0000	0.0188	0.0000	0.0213	0.0000
12	0.0178	0.0000	0.0159	0.0000	0.0194	0.0000	0.0221	0.0000
13	0.0194	0.0001	0.0173	0.0001	0.0194	0.0000	0.0247	0.0000
14	0.0195	0.0003	0.0173	0.0001	0.0195	0.0000	0.0258	0.0000
15	0.0202	0.0003	0.0196	0.0001	0.0196	0.0000	0.0270	0.0000
16	0.0209	0.0004	0.0203	0.0002	0.0225	0.0000	0.0310	0.0000
17	0.0232	0.0006	0.0210	0.0003	0.0234	0.0000	0.0312	0.0000
18	0.0233	0.0006	0.0244	0.0011	0.0264	0.0000	0.0314	0.0000
19	0.0276	0.0009	0.0276	0.0332	0.0302	0.0000	0.0316	0.0000
20	0.0318	0.0025	0.0289	0.0999	0.0304	0.0000	0.0318	0.0000
21	0.0320	0.0030	0.0336	0.1669	0.0320	0.0010	0.0320	0.0000
22	0.0407	0.0038	0.0400	0.1939	0.0407	0.0045	0.0407	0.0000
23	0.0505	0.2973	0.0495	0.2695	0.0505	0.0047	0.0436	0.0000
24	0.0552	2.8838	0.0738	0.9778	0.0552	0.4326	0.0471	0.0000
25	0.0873	2.9644	0.1455	2.6484	0.0558	0.8335	0.0686	0.0000
26	0.1500	4.0016	0.1500	3.5130	0.0762	2.7182	0.1021	0.0000
27	0.5333	9.9369	0.1548	3.5891	0.1548	4.0375	0.2000	0.0000
28	4.8000	12.7530	0.6000	10.4479	0.6000	6.5259	0.2087	0.0000

TABLE 2

Ordered \mathcal{P} -values of the statistics $\tanh^{-1} |\hat{R}_{YX}(\omega)|$ for testing the relevancy of $Y(t)$ in $Z(t) = (X(t)', Y(t))'$ at a level of significance $\alpha = 5\%$ and $|R_{YX}^0|^2 = 0.31$. Boldfaced numbers correspond to hypotheses that are not rejected.

j	α_j	$Z_1(Z_2 Z_3)$	α_j	$Z_2(Z_1 Z_3)$	α_j	$Z_3(Z_1 Z_2)$
1	0.0125	0.0145 [3, 0]	0.0125	0.0000 [3, 0]	0.0125	0.0001 [3, 0]
2	0.0136	0.0423 [3, 1]	0.0136	0.0000 [3, 1]	0.0136	0.0006 [3, 1]
3	0.0146	0.4230 [3, -1]	0.0146	0.0002 [3, -1]	0.0146	0.0076 [4, 2]
4	0.0157	1.8357 [1, 0]	0.0157	0.0002 [3, 2]	0.0150	0.0585 [4, 1]
5	0.0175	1.8700 [3, 2]	0.0161	0.0126 [4, 2]	0.0161	0.1442 [4, 3]
6	0.0180	2.9918 [4, 0]	0.0166	0.0269 [4, 1]	0.0162	0.2126 [3, -1]
7	0.0205	2.9974 [2, 0]	0.0180	0.4077 [4, 0]	0.0175	0.9002 [3, 2]
8	0.0238	3.6706 [1, 1]	0.0204	0.4496 [2, -3]	0.0180	1.1483 [4, 0]
9	0.0268	3.7021 [1, -1]	0.0205	0.4619 [3, -2]	0.0205	2.3917 [1, 0]
10	0.0308	4.1276 [4, -1]	0.0212	0.5470 [4, 3]	0.0238	2.9965 [2, 0]
11	0.0361	4.1487 [4, 1]	0.0213	1.0933 [4, -1]	0.0282	3.1107 [4, -1]
12	0.0436	4.1715 [2, -1]	0.0238	2.0798 [4, -2]	0.0327	3.1378 [1, -1]
13	0.0552	4.1737 [2, 1]	0.0247	2.9126 [2, 0]	0.0387	3.7724 [2, -1]
14	0.0750	5.1549 [3, -2]	0.0296	2.9696 [1, 0]	0.0475	3.9966 [1, 1]
15	0.0857	11.5939 [4, -2]	0.0369	3.3153 [2, -1]	0.0615	4.1726 [2, 1]
16	0.1000	11.8675 [4, 2]	0.0449	3.9879 [1, 1]	0.0873	6.2193 [2, -2]
17	0.1200	11.9624 [1, -2]	0.0571	3.9979 [2, -2]	0.1021	7.7272 [4, -2]
18	0.1500	11.9950 [2, -2]	0.0632	4.1589 [2, 1]	0.1231	10.1307 [3, -2]
19	0.2000	11.9969 [1, 2]	0.0906	4.1702 [1, -1]	0.1548	11.4418 [1, 2]
20	0.3000	11.9989 [2, 2]	0.1600	5.3440 [3, 3]	0.2087	11.9930 [1, -2]
21	0.6000	21.7430 [3, 3]	0.1655	11.3474 [1, 2]	0.3200	11.9992 [2, 2]
22	0.6857	36.8728 [3, -3]	0.2286	11.9466 [2, 2]	0.6857	17.4992 [2, -3]
23	0.8000	82.8161 [1, -3]	0.3692	11.9978 [1, -2]	0.8000	50.3377 [4, -3]
24	0.9600	90.1962 [2, -3]	0.9600	15.4016 [3, -3]	0.9600	56.6169 [3, 3]
25	1.2000	94.2370 [4, 3]	1.2000	25.0787 [4, -3]	1.2000	90.1846 [1, 3]
26	1.6000	95.3323 [4, -3]	1.6000	89.8438 [1, -3]	1.6000	95.2743 [3, -3]
27	2.4000	95.5611 [2, 3]	2.4000	93.3461 [2, 3]	2.4000	95.8520 [2, 3]
28	4.8000	95.9988 [1, 3]	4.8000	94.6360 [1, 3]	4.8000	95.9983 [1, -3]

Table 2 that at this level of significance, H is retained for testing the relevancy of the sensor with output $Z_1(t)$ and rejected for the sensors with outputs $Z_2(t)$ and $Z_3(t)$, respectively. Under the conditions given in section 4, the optimum position found in this experiment is that proposed by the manufacturer. However, this proposal was based on detecting knock by considering the lowest mode ($P = 1$) only. We found that in this case the hypothesis H is retained at a level of significance $\alpha = 5\%$ only for the sensor with output $Z_2(t)$ when $|R_{YX}^0|^2 = 0.01$. We note from Table 2 that the latter does not perform better than the sensor with output $Z_3(t)$.

The results found are coherent with those reported in [28]. The use of other weights, for example Hanning, Hamming etc., does not substantially alter the results. In [35] the ordinary sequentially rejective Bonferroni test has been applied for testing simultaneously the smallness of coherence for the three rotation speeds 1 750, 3 500 and 5 250 rpm and four mode frequencies. The relevancy decisions are similar to the ones presented here.

5.3. KNOCK DETECTION

The parametric detector had been implemented in a DSP-based system capable of real-time operation for one cylinder at engine speed of 6 000 rpm and more. To assure analysis of exactly the same cycles used to identify optimum sensor positions, data was taken from a file rather than from an A/D converter. Computations were performed with 16 bit fixed-point accuracy at a processor cycle time of 125 ns. The first 50 combustion cycles were used to initialize adaptive weighting functions before

analyzing the complete data file. For our experiments, we have chosen various combinations of resonance frequencies and intervals of crank angles. Results are shown for $10^\circ \leq \gamma \leq 40^\circ$ and frequency sets f_1 to f_4 , f_2 to f_4 , and f_1 to f_3 . Theoretical probabilities of false alarms are 1 % and 5 %. Detector decisions have been compared with the reference list mentioned above and from this, we computed the numbers of right and false decisions on knock. They are shown in Table 3, where results for 1 % are given in the upper half and those for 5 % in the lower half, respectively.

Results for the 1 % level of false alarms indicate that sensor output $Z_4(t)$ is the worst one under any condition. A ranking of the other sensors is difficult because it depends on the costs of false alarms and missing detection of knock. However, there are some interesting points to note. Results for $Z_1(t)$ become very bad if the fourth resonance at f_4 is missing. A similar effect can be seen for $Z_2(t)$ and frequency f_1 . This could be expected from the results of testing relevancy presented above. The best results of $Z_3(t)$ are reached for frequencies f_1 to f_4 . On the other hand, the superiority of $Z_1(t)$ for frequencies f_1 to f_4 , as established by the tests, is not verified by the results of Table 3. This may be due to the relatively small number of cycles that have been used. For an effective adaptation of the weighting functions in the time and frequency domain a number of cycles greater than 50 is preferred. In addition, data dependent inaccuracies caused by fixed-point arithmetic may degrade performance. Results for a theoretical rate of false alarms of 5 % are quite similar but ranking is even more difficult. It is interesting to note that $Z_1(t)$ shows a significant increase of the number of right decisions on knock as well as of that of false alarms. This effect may be related to the adaptation of some parameters of the detector that depend on the result of the test for knock and acts like a feedback loop. The same effect may be seen for other sensor outputs at different thresholds.

TABLE 3

Results of knock detection with a 16 bit fixed-point digital signal processor. Theoretical probability of false alarm : 1.0 % (upper half) and 5.0 % (lower half).

Decision on Knock	Sensor Output				Resonance Frequencies
	$Z_1(t)$	$Z_2(t)$	$Z_3(t)$	$Z_4(t)$	
Right	2	4	3	0	f_1 to f_4
False	0	1	0	0	
Right	2	4	0	0	f_2 to f_4
False	0	2	0	1	
Right	0	3	2	0	f_1 to f_3
False	0	1	0	0	
Right	9	4	3	4	f_1 to f_4
False	24	2	2	12	
Right	8	6	6	4	f_2 to f_4
False	26	3	2	15	
Right	9	5	3	5	f_1 to f_3
False	20	3	2	14	

6. Conclusions

We have presented a method for testing the relevancy of sensors in an arbitrary group of sensors for the detection of knock in spark ignition engines. By using a linear prediction filter approach, we have investigated the multiple coherence and shown that its closeness to zero at some frequencies is a measure for the relevancy of the sensor under consideration. We have estimated the multiple coherence from spectral estimates and pointed out the difficulty to use it as a test statistic. From an analogy of the multiple coherence to the squared multiple correlation coefficient and, considering known results about the latter, we have used a suitable statistic for testing multiple coherences at different frequencies simultaneously. Due to its simplicity, we have applied the generalized sequentially rejective Bonferroni test. Our principal result is that sensor relevancy decisions depend on the consideration of higher resonance frequencies. The simultaneous relevancy test suggests a position also proposed by the engine manufacturer. However, this position is not optimum for the knock detectors in use because these detectors only consider the first resonance frequency. For the optimization of sensor positions, the resonance frequencies have to be known accurately. This knowledge can be gained from the analysis of the cylinder pressure signal. Therefore, data acquisition has to take place on a test bed. This is not an obstacle because optimum sensor positions are specific to an engine type and have to be found once. To emphasize the usefulness of tests on relevancy, we have performed experiments with a fixed-point digital signal processor. The results show that the performance of knock detectors strongly depends on the frequencies chosen for analysis as well as on the position of the sensor. This effect is noticeable even for 16 bit fixed-point arithmetic. It may be concluded that improved performance is gained by proper choice of frequencies and sensor positions and that these improvements are worth.

Manuscrit reçu le 6 décembre 1990.

ACKNOWLEDGEMENTS

The authors wish to thank Prof. J. F. Böhme for his valuable comments and suggestions.

REFERENCES

- [1] H. DECKER and H.-U. GRUBER, Knock Control of Gasoline Engines — A Comparison of Solutions and Tendencies, with Special Reference to Future European Emission Legislation, *SAE Technical Paper Series*, 850298, Warrendale, PA, 1985.
- [2] A. FELSKE and G. HOPPE, Detection of Knocking Centres by Holographic Vibration Analysis, *Proc. VW-Symposium « Knocking of Combustion Engines »*, Wolfsburg, FRG, 1981.

- [3] B. STOFFREGEN, Applications of Holography and Laser-Doppler Techniques for Vibration Analysis (in German), *VDI Berichte*, **617**, 145-167, Düsseldorf, FRG, 1986.
- [4] R. N. JANEWAY, Combustion Control by Cylinder-Head Design, *S.A.E. Journal*, **XXIV(5)**, 498-513, May 1929.
- [5] P. KREUTER, B. GAND, W. BICK, and F. PISCHINGER, Einflüsse der Brennraumgrundform, des Verdichtungsverhältnisses und des Zylinderhubvolumens auf den Prozeßverlauf im Ottomotor bei verschiedenen Hub-Bohrungsverhältnissen (in German), in *Motorische Verbrennung*, Sonderforschungsbereich 224 der RWTH Aachen, 23-39, October 1988.
- [6] K. LÖHNER and H. MÜLLER, Gemischbildung und Verbrennung im Ottomotor (in German), in H. List, editor, *Die Verbrennungskraftmaschine*, volume 6, Springer-Verlag, Vienna, 1967.
- [7] F. PISCHINGER, H.-P. KOLLMEIER, and U. SPICHER, Das Klopfen im Ottomotor — Ein altes Problem aus neuer Sicht (in German), in *Der Arbeitsprozeß des Verbrennungsmotors*, 17-34, Graz, April 1987.
- [8] U. SPICHER, H.-P. KOLLMEIER, and H. KRÖGER, Erfassung klopfender Verbrennung mit Hilfe der Lichtleitertechnik (in German), in *Motorische Verbrennung*, Sonderforschungsbereich 224 der RWTH Aachen, 40-57, October 1988.
- [9] J. H. CURRIE, D. S. GROSSMAN, and J. J. GUMBLETON, Energy conservation with increased compression ratio and electronic knock control, *SAE Technical Paper Series*, **790173**, Warrendale, PA, 1979.
- [10] C. M. ANASTASIA and G. W. PESTANA, A Cylinder Pressure Sensor for Closed Loop Engine Control, *SAE Technical Paper Series*, **870288**, Warrendale, PA, 1987.
- [11] N. COLLINGS, S. DINSDALE, and D. EADE, Knock Detection by means of the Spark Plug, *SAE Technical Paper Series*, **860635**, Warrendale, PA, 1986.
- [12] K. WENZLAWSKI and D. HEINTZEN, Ionenstrommessung an Zündkerzen von Ottomotoren als Klopfkennungsmittel (in German), *MTZ Motortechnische Zeitung*, **51(3)**, 118-122, 1990.
- [13] T. PRIEDE and R. K. DUTKIEWICZ, The Effect of Normal Combustion and Knock on Gasoline Engine Noise. In *Proceedings of the 1989 Noise and Vibration Conference*, number P-222, Society of Automotive Engineers, May 1989.
- [14] N. HÄRLE, *Analyse, Modellbildung und Detektion von Klopfsignalen im Körperschall von Ottomotoren* (in German), Fortschritt-Berichte VDI 11, Nr. 113. VDI-Verlag, Düsseldorf, FRG, 1989.
- [15] R. HICKLING, D. A. FELDMAIR, F. H. K. CHEN, and J. S. MOREL, Cavity Resonances in Engine Combustion Chambers and Some Applications, *Journal of the Acoustical Society of America*, **73(4)**, 1170-1178, April 1983.
- [16] E. SKUDRZYK, *The Foundations of Acoustics*, Springer-Verlag, Vienna, New York, 1971.
- [17] N. HÄRLE and J. F. BÖHME, Detection of Knocking for Spark Ignition Engines Based on Structural Vibrations, *Proceedings of IEEE International Conference on Acoustics, Speech, and Signal Processing*, Dallas, TX, 1987.
- [18] D. R. BRILLINGER, *Time Series: Data Analysis and Theory*, Expanded Ed., Holden-Day, San Francisco, 1981.
- [19] N. N., Control of knock improved, *Automotive Engineering*, **96(1)**, 65-69, January 1988.
- [20] Th. M. BOSSMEYER and J. F. BÖHME, Parametric detectors for knock in spark ignition engines, in W. Ameling, editor, *Proceedings of 7. Aachener Symposium für Signaltheorie*, number 253 in Informatik-Fachberichte, September 1990.
- [21] N. L. JOHNSON and S. KOTZ, *Continuous Univariate Distributions-1*, John Wiley & Sons, New York, 1970.
- [22] A. FELSKE and A. HAPPE, Vibration Analysis by Double Pulsed Laser Holography, *SAE International Automotive Engineering Congress and Exposition*, **770030**, Cobo Hall, Detroit, 1977.
- [23] E. L. LEHMANN, *Testing Statistical Hypotheses*, 2nd. Edition, John Wiley & Sons, New York, 1986.
- [24] N. R. GOODMAN, Statistical Analysis Based Upon a Certain Multivariate Complex Gaussian Distribution (An Introduction), *Ann. Math. Statist.*, **34**, 152-177, 1963.
- [25] D. E. AMOS and L. H. KOOPMANS, Tables of the Distribution of the Coefficient of Coherence for Stationary Bivariate Gaussian Processes, *Sandia Corporation Monograph*, SCR-483, 1963.
- [26] G. W. GROVES and E. J. HANNAN, Time Series Regression of Sea Level on Weather, *Rev. Geophysics*, **6**, 129-174, 1968.
- [27] T. W. ANDERSON, *An Introduction to Multivariate Statistical Analysis*, second edition, John Wiley & Sons, New York, 1984.
- [28] A. M. ZOUBIR and J. F. BÖHME, Simultaneous Tests for Optimizing Sensor Positions in Knock Detection, *Proc. EUSIPCO Barcelona*, 285-288, 1990.
- [29] Y.-S. LEE, Results on the Sampling Distribution of the Multiple Correlation Coefficient, *J. R. Stat. Soc.*, **B, 33**, 117-130, 1971.
- [30] R. A. FISHER, The General Sampling Distribution of the Multiple Correlation Coefficient, *Proceedings of the Royal Society of London, Series A*, **121**, 654-673, 1928.
- [31] L. D. ENOCHSON and N. R. GOODMAN, Gaussian approximations to the distribution of sample coherence. *Tech. Rep. AFFDL-TR-65-67*, Wright-Patterson Air Force Base, 1965.
- [32] S. HOLM, A simple sequentially rejective multiple test procedure, *Scandinavian Journal of Statistics*, vol. 6, 65-70, 1979.
- [33] Y. HOCHBERG and A. C. TAMHANE, *Multiple Comparison Procedures*, John Wiley & Sons, New York, 1987.
- [34] E. PARZEN, On Empirical Multiple Time Series Analysis, in *Proc. Fifth Berkeley Symp. Math. Statist. Prob.*, 1, Eds. Le Cam and J. Neyman, 305-340, Berkeley: Univ. of Cal. Press, 1967.
- [35] H. HÖVELS, *Varianzstabilisierende Transformationen und Testen auf Irrelevanz von Körperschallsensoren bei Ottomotoren* (in German), diploma thesis, Lehrstuhl für Signaltheorie, Ruhr-Universität Bochum, FRG, March 1990.